On-Chip Double Emulsion Droplet Assembly for Laser-Target Fabrication

Introduction

Inertial confinement fusion (ICF) experiments use spherical organic polymer shells as mandrels for cryogenic foam targets. The targets are typically fabricated by polymerizing double-emulsion (DE) shells and then voiding the inner fluids.[1,2] In this process, special care must be taken to ensure DE droplet uniformity because fusion experiments impose rigid requirements on the sphericity and wall thickness uniformity of foam targets.

Up to the present, the formation of uniform DE droplets has relied mainly on the controlled merging of two immiscible fluids.[1–5] DE droplets for target fabrication are currently prepared using a triple-orifice droplet generator.[1] This method generates remarkably monodisperse emulsions with good uniformity. The DE droplet size, however, is constrained by the device dimensions, and the microfluidic devices need to be recalibrated and tuned to the correct dimensions each time they are used. In this article, we propose a DE assembly line based on a "lab-on-a-chip" droplet generator, where individual water and oil droplets generated from an on-chip dispensing system are combined directly to form DE's. As a droplet-based microfluidic system, this scheme has the advantages of reconfigurability, flexibility, and scalability.

Background

Because the formation of DE droplets in air requires combining at least one aqueous (water) and one non-aqueous (oil) liquid droplet, we use electrowetting-on-dielectric (EWOD) and dielectrophoresis (DEP) simultaneously to dispense and transport water and oil droplets, respectively. Because all actuation is electrical, we can program each step and, in this way, obtain maximum operational flexibility.

1. Electrowetting-on-Dielectric (EWOD)

The electrowetting effect describes the observable influence of an electric field on both bulk liquid motions and the contact angle. The motive force is due to the response of the free electric surface charge to the electric field.[6,7] In an EWOD-based microfluidic device as shown in Fig. 123.43, droplets are sandwiched between parallel plates and manipulated by applying voltages to a series of adjacent electrodes on the bottom. A wide variety of fundamental fluid operations have been realized using EWOD. These operations include droplet transport,[8] dispensing,[9–11] separation,[9,11] coalescence,[9] dilution,[12] and others.

2. Dielectrophoresis (DEP)

The dielectrophoretic (or DEP) force is the force exerted on dielectrics when subjected to a nonuniform electric field.[13,14] As another extensively studied mechanism for droplet manipulation, DEP is useful for manipulating insulating, polarizable media. For example, decane cannot be moved by EWOD[15] but can be moved by DEP.[16]

EWOD and DEP are two observable effects of liquid under electrostatic fields, both of which are electromechanical in nature. Jones[7] first clarified the frequency-dependent relationship between these two mechanisms. For a liquid with finite electrical conductivity and dielectric constant, there exists a critical frequency that separates conductive (EWOD) and dielectric (DEP) behavior.[7,17,18] In the high-frequency limit, the liquid behaves as an insulator so that the electric field penetrates it. As a result, the observable electromechanical response of the liquid is virtually identical to liquid DEP.

3. General Microfluidic Platform Based on EWOD and DEP

The combination of droplet-based EWOD and DEP microfluidics makes it possible to manipulate both conductive and insulating droplets on the same chip. Conceptually, such a combination of EWOD and DEP may be visualized with the parallel-plate scheme shown in Fig. 123.43. The device consists of two parallel glass plates: a bottom plate that consists of a patterned array of individually addressable electrodes, and a top plate that is a continuous ground electrode. Usually the bottom plate is coated with a dielectric layer, and both the top and bottom surfaces are covered with a thin hydrophobic film to decrease the surface wettability.

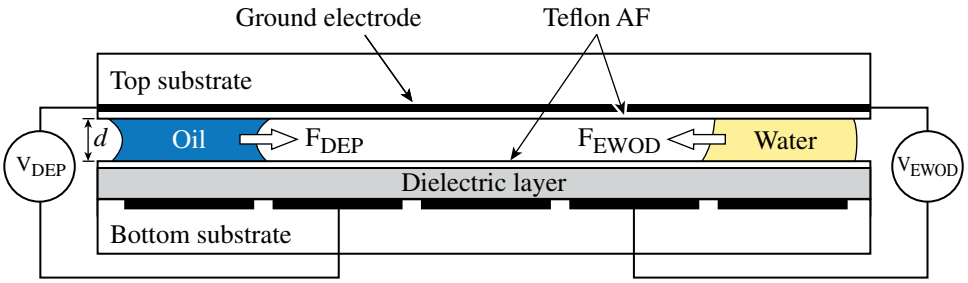

Figure 123.43
Cross section of a parallel-plate device containing a dielectric layer on the bottom plate to manipulate oil and water droplets by DEP and EWOD, respectively.

Microfabrication and Experiments

The basic features of the droplet-based microfluidic system are illustrated in a cross-sectional view in Fig. 123.43. The bottom glass substrate is evaporatively coated with 100 nm of aluminum and then photolithographically patterned into a two-dimensional electrode array. The structure is then spin coated with 0.5 μm of spin-on-glass (SOG) (Futurrex IC1-200) as the dielectric layer and 1 μm of amorphous fluoropolymer (DuPont Teflon-AF) as a hydrophobic coating. The top plate is a glass plate with a transparent indium tin oxide layer as a ground electrode covered by 1 μm of Teflon-AF as a hydrophobic coating.

The top substrate is positioned above the bottom substrate by appropriate spacers. Voltages applied to individual electrodes are controlled by a LabView-based controller. It is important to recognize that different voltages are applied for EWOD actuation and DEP actuation. For EWOD actuation, dc or low-frequency ac voltage, typically <100 V, is employed. For oil DEP actuation, dc or ac voltage (50 to 100K Hz) is used, but usually >250 V.

Droplet-Dispensing Reproducibility

In a typical dispensing operation, a liquid finger is drawn from a large reservoir droplet. Liquid pinch-off occurs by activating the electrode at the front end of the liquid finger and the reservoir electrode and deactivating the electrodes in between (the cutting electrode) until the liquid front is separated from the liquid bulk. Successful pinch-off requires an application of electrode voltages above some threshold value.[6] The sequence of steps of droplet dispensing is shown in Fig. 123.44. EWOD-based water droplet dispensing has been widely studied,[9–11] but dielectric-droplet (oil) dispensing has not received much attention. Here we demonstrate repeatable dielectric droplet dispensing on a microfluidic chip as shown in Fig. 123.44. Because of the difference in the electric-actuation mechanism, oil-droplet manipulation by DEP requires much higher voltages than EWOD dispensing of aqueous droplets.

Dispensing reproducibility is of paramount importance in laser-target fabrication because the uniformity of subsequently formed DE droplets is largely determined by the initial liquid volume control. The requirements for double emulsion droplet uniformity are described in **Appendix A** (p. 156). It has been observed that the final extracted drop volume is usually somewhat larger than the volume subtended by a square electrode (volume = a^2d, where a is the length of a square electrode in the electrode array and d is the spacing between bottom and top substrates).[11] The reason is that a liquid tail formed after separation adds some additional liquid to the already-formed

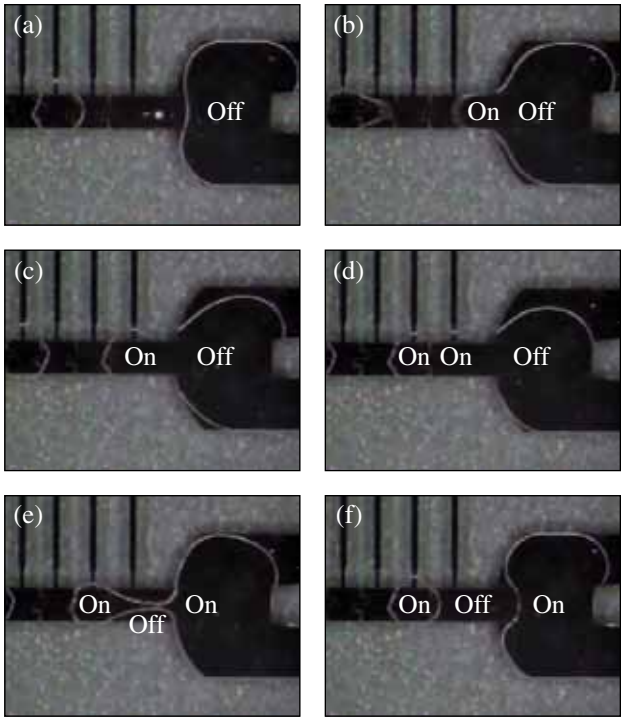

Figure 123.44
Top view of an on-chip dispenser showing the sequence of a silicone oil droplet being formed. (a) The reservoir and an already-formed droplet; (b)–(d) the liquid finger is formed, and, meanwhile, the first droplet is delivered away; (e) the pinch-off occurs; (f) a new droplet is formed.

droplet. It is this volume that produces variability in the dispensing operation. In this research we investigated the effects of applied voltage and electrode shape on droplet volume control for an on-chip dispensing system because they both impact the tail volume directly.

1. Effect of Applied Voltage on Droplet Volume Variations

We investigated the dependence of dispensed water drop volume on the actuation voltage in a structure with 1-mm-sq electrodes. The droplet volume becomes sensitive when the applied voltage is close to the minimum required value for pinch-off. For example, when applied voltage decreased from 62.5 V to the minimum pinch-off voltage of 55.0 V, the droplet volume dropped by almost 30% as shown in Fig. 123.45. The same result is observed with both square and circular dispensing electrodes. The voltage effect is a result of the effect on the tail shapes during pinch-off. As shown in Fig. 123.46, a smaller tail is observed at lower voltage, and the pinch-off position also moves closer to the individual droplet. The shape of the tail changes because the liquid finger necking depends on the electrowetting force, which is directly related to applied voltage.[6]

Figures 123.46(c) and 123.46(e) show that with square electrodes, a smaller area of the dispensing electrode is filled by liquid during pinch-off at lower voltage. This smaller finger front may also contribute to reduced dispensed-droplet volume. No obvious change in the finger front is observed for circular electrode structures, as shown in Figs. 123.46(g) and 123.46(i), but the droplet volume remains very sensitive to voltage change. In general, the tail volume plays the most important role in determining variation in droplet volume.

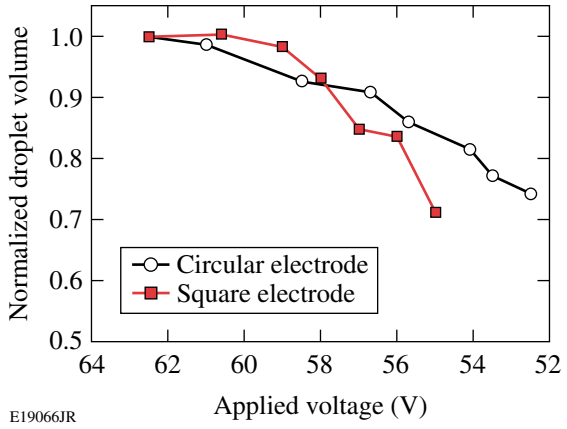

Figure 123.45
The normalized volume variation of a series of droplets generated by different applied voltages. All tests were done with DI water. The gap between the top and bottom substrates was 85 μm, and the voltage applied was 100 Hz ac.

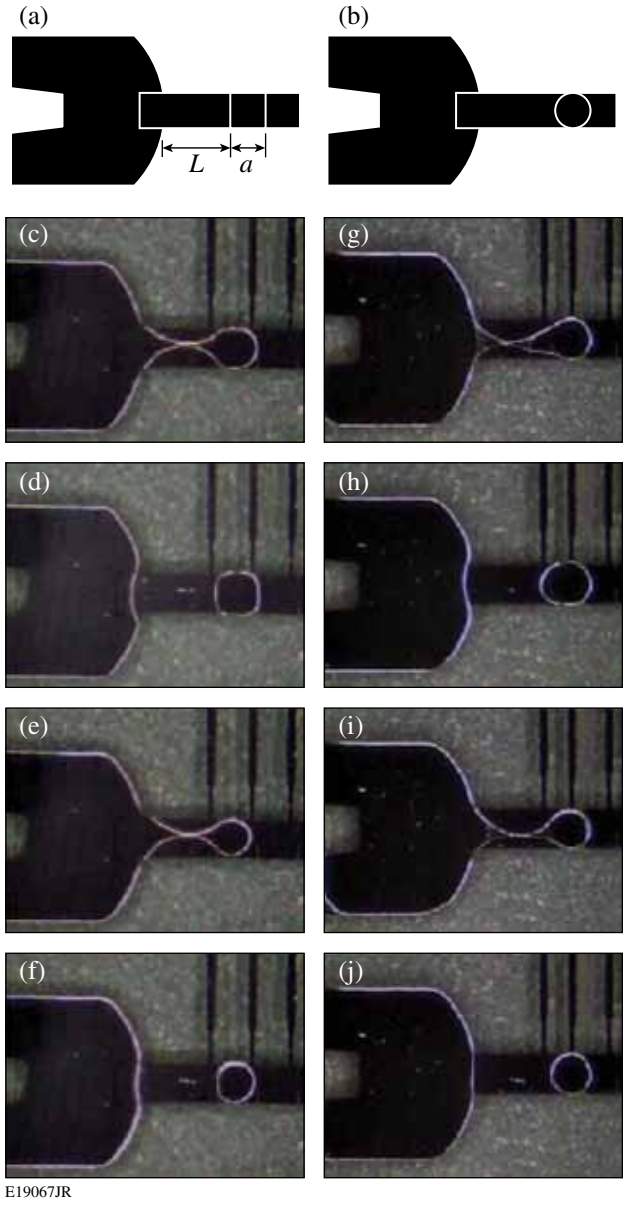

Figure 123.46
The effect of applied voltage on droplet volume variation. [(a),(b)] Square and circular dispensing electrodes used for the dispensing experiments. The square electrode is 1 mm × 1 mm and the diameter of the circular electrode is 1 mm. The length of the cutting electrode is 2 mm. [(c),(d)] Pinch-off and the formed droplet on the square electrode by applying 62.5-V_{rms}, 100-Hz ac voltage; [(e),(f)] pinch-off and the formed droplet on the square electrode by applying 55-V_{rms}, 100-Hz ac voltage; [(g),(h)] pinch-off and the formed droplet on the circular electrode by applying 62.5-V_{rms}, 100-Hz ac voltage; [(i),(j)] pinch-off and the formed droplet on the circular electrode by applying 52.5-V_{rms}, 100-Hz ac voltage. In all cases, the gap between top and bottom substrates is 85 μm.

2. Effect of Cutting Electrode on Droplet Volume and Reproducibility

We tested electrode structures with different cutting electrode length (L) to investigate its effect on droplet volume and reproducibility. As shown in Fig. 123.47, the dispensed droplet volume increases directly with L. Droplets with an average volume of 103 nL and 183 nL were dispensed on a 1-mm × 1-mm-sq electrode using cutting electrodes of lengths $L = 2$ mm and 3 mm, respectively. These droplet volumes are greater than the volume subtended by one electrode (85 nL). The increase in droplet volume is due to the larger tail formed on longer cutting electrodes during pinch-off. Similar behavior is also observed on 2-mm × 2-mm-sq electrodes.

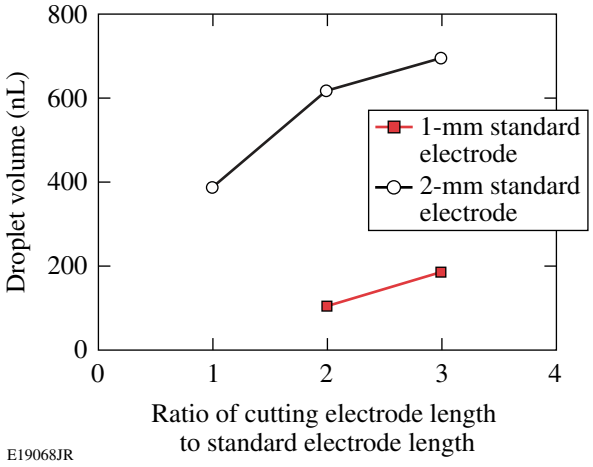

Figure 123.47
Average droplet volume versus cutting electrode length. All tests were performed with DI water. The gap between top and bottom substrates was 85 μm, and 90-V_{rms}, 100-Hz ac voltage was applied.

Droplet volume reproducibility suffers as L is increased. As indicated in Fig. 123.48 and Table 123.V, the coefficient of variation (CV = standard deviation/mean) increases significantly when the ratio of the cutting electrode length to standard electrode length (L/a) approaches $L/a = 3$. The reason for this behavior is the reduced influence of the cutting electrode on the radius of curvature in the pinch-off region. In fact, the pinch-off position becomes indeterminate for sufficiently large L/a. Large droplet volume variation (CV = 40%) is observed when $L/a = 3$ on a 2-mm × 2-mm electrode because of the instability of the pinch-off position (see Fig. 123.49).

The best reproducibility (CV = 3.0%) is achieved for a cutting electrode of the same length as that of the standard electrodes. This reproducibility is adequate for laser target fabrication (see **Appendix A**, p. 156, for detailed discussion).

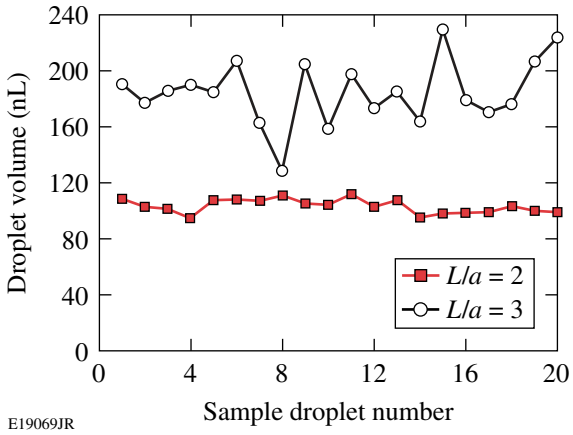

Figure 123.48
Droplet volume variation for two lengths of the cutting electrode. All tests were performed with DI water on 1-mm × 1-mm dispensing electrodes. The gap between the top and bottom substrates was 85 μm, and 90-V_{rms}, 100-Hz ac voltage was applied.

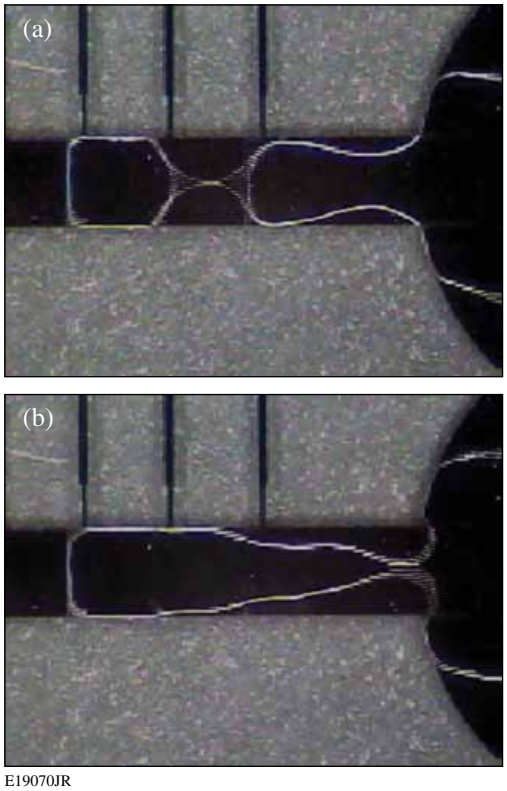

Figure 123.49
Instability of the pinch-off position for a droplet dispensing on a 2-mm standard electrode and a 6-mm cutting electrode. The gap between the top and bottom substrates was 85 μm, and 90-V_{rms}, 100-Hz ac voltage was applied.

Table 123.V: Effect of cutting electrode length on volume reproducibility (CV) for droplets dispensed on 1-mm and 2-mm dispensing electrodes and an 85-μm channel gap. In all cases, the voltage applied was 90 V_{rms}, 100 Hz ac.

Electrode size	$L/a = 1$	$L/a = 2$	$L/a = 3$
1 mm × 1 mm	—	4.7%	12.7%
2 mm × 2 mm	3.0%	5.3%	40%

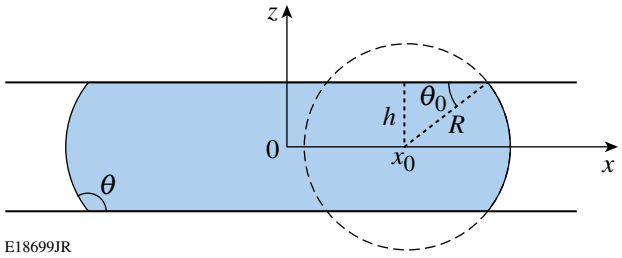

Figure 123.50
Droplet geometry when sandwiched between parallel plates.

On-Chip Double Emulsion Formation

1. Gibbs Free Energy Model

When two immiscible droplets are brought together, a DE droplet forms spontaneously if the Gibbs free energy is reduced by the emulsification process. The Gibbs surface energy change between initial and final states of a DE formation process is

$$\Delta G = G_{DE} - (G_{water} + G_{oil}), \tag{1}$$

where G_{DE} is the total Gibbs interfacial energy of a DE droplet and G_{water} and G_{oil} are Gibbs surface energies of the individual water and oil droplets forming that DE droplet. The Gibbs energy change ΔG is a convenient criterion for testing the likelihood of DE formation. A negative ΔG means the DE formation is favored. In the following, we develop a simple model to calculate the Gibbs surface energy changes associated with double emulsion formation.

The Gibbs surface energy is a sum of the product of interfacial tensions and corresponding surface areas. The surface shape of a droplet sandwiched between parallel plates is strongly affected by the contact angle against the substrate and the spacing between top and bottom substrates. For the geometry model shown in Fig. 123.50, the droplet volume is

$$V = 2\int_0^h \pi x^2 \,\mathrm{d}z$$

$$= 2\pi\left[\left(x_0^2 + R^2\right)h - \frac{1}{3}h^3 + 2x_0R^2\left(\frac{1}{2}\theta_0 + \frac{1}{4}\sin 2\theta_0\right)\right], \tag{2}$$

where the spacing between substrates is 2 h, $\theta_0 = \theta - \pi/2$, θ is the contact angle on a hydrophobic surface ($\theta > 90°$), and $R = -h/\cos\theta$.

The lateral surface area and base areas are then

$$S_L = 2\int_0^{\theta_0} 2\pi(x_0 + R\cos\theta')R\,\mathrm{d}\theta'$$

$$= 4\pi R(x_0\theta_0 + R\sin\theta_0), \tag{3}$$

$$S_B = 2\pi(x_0 + R\cos\theta_0)^2. \tag{4}$$

When $\theta < 90°$, droplet volume and droplet surfaces can be derived as

$$V = 2\pi\left[\left(x_0^2 + R^2\right)h - \frac{1}{3}h^3 - 2x_0R^2\left(\frac{1}{2}\theta_0 + \frac{1}{4}\sin 2\theta_0\right)\right], \tag{5}$$

$$S_L = 2\int_0^{\theta_0} 2\pi(x_0 - R\cos\theta')R\,\mathrm{d}\theta'$$

$$= 4\pi R(x_0\theta_0 - R\sin\theta_0), \tag{6}$$

$$S_B = 2\pi(x_0 - R\cos\theta_0)^2, \tag{7}$$

where $\theta_0 = \pi/2 - \theta$ and $R = h/\cos\theta$.

Several studies[19,20] have reported that, for a water-in-oil DE droplet in the parallel-plate structure, the oil becomes entrapped underneath the inner water droplet as illustrated in Fig. 123.51(b). We analyzed the Gibbs surface energy change for both cases of the water droplet resting on the Teflon surface and the water droplet on a thin layer of oil. Using Eqs. (2)–(7) and the interfacial tension data shown in Table 123.VI, we calculate ΔG for water-in-silicone oil (20 cst) DE for the configurations of Figs. 123.51(a) and 123.51(b). ΔG per unit total liquid volume is expressed as the ratio of the volume of water to the total volume of water and oil in the DE. Both configurations give $\Delta G < 0$, but the configuration with the oil entrapped underneath the water system is energetically favored.

As noted above, a water droplet and an oil droplet usually combine to form a water-in-oil DE because water has a higher surface tension than most oils, but we can reverse this tendency if we add surfactant Silwet L-77 to the water. The interfacial tension for Silwet-treated water (at the surfactant concentration of 0.0625 wt%, listed in Table 123.VI) is greater than silicone

oil, but lower than mineral oil. Therefore it is not effective to choose silicone oil for oil-in-water DE's. Instead, we chose mineral oil and then calculated ΔG for water treated with mineral oil–in–Silwet as a function of the volume ratio of mineral oil.

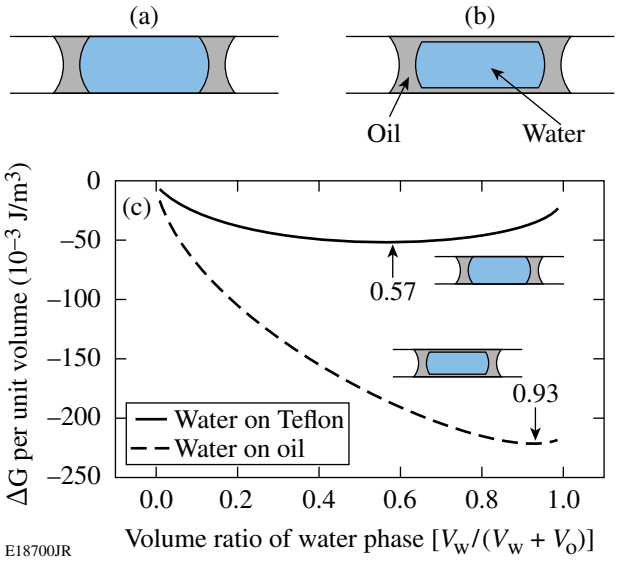

Figure 123.51
Water-in-silicone oil (20 cst) DE droplet in the parallel-plate structure: (a) the inner water droplet rests on the Teflon surface; (b) the inner water droplet rests on a thin layer of oil; (c) ΔG of DE formation for both cases (a) and (b).

Table 123.VI: Interfacial tension data at room temperature (mN/m).

Interface	Interfacial tension
Water/air	74
Silicone oil (20 cst)/air	20.6
Mineral oil/air	28.1
Silicone oil (20 cst)/water	35
Mineral oil/water	49
Water/Teflon™	49
Silicone oil (20 cst)/Teflon™	5.6
Mineral oil/Teflon™	10.25
Teflon™/air	18
W_{S-t}/air	24.7
Mineral oil/W_{S-t}	4.5
W_{S-t}/Teflon™	2.46

W_{S-t}: Silwet-treated water (0.0625 wt%)

As shown in Fig. 123.52, the requirement for DE formation, ΔG < 0, is met. Similar to water-in-oil DE's, one might also wonder whether a thin layer of water could be entrapped underneath the oil droplet. To test for this possibility, we calculated ΔG for both this case and the case of oil resting directly on Teflon surface. Figure 123.52 shows that the energy is minimized when the inner oil droplet is separated from the Teflon surface by a layer of water. We have some evidence for this configuration but further experimental verification is needed.

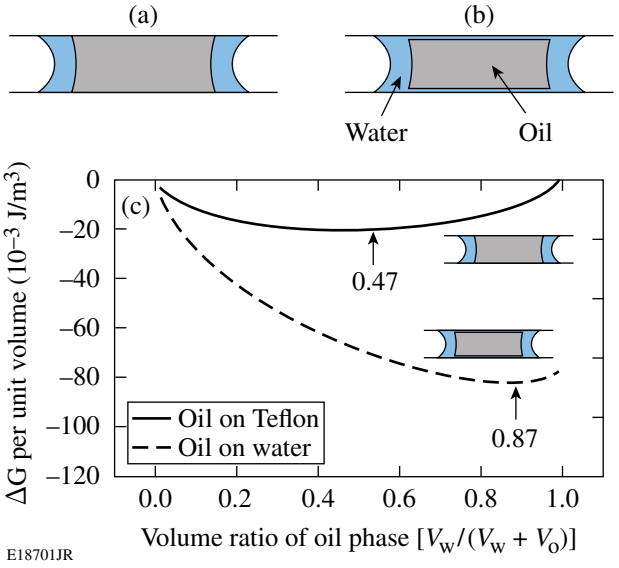

Figure 123.52
Mineral oil–in–Silwet-treated-water DE formation in parallel plates; (a) the inner oil droplet rests on the Teflon surface; (b) the inner oil droplet rests on a thin layer of water; (c) ΔG of DE formation for both cases (a) and (b).

2. Experiments for Water-in-Oil DE Formation

We tested the electric-field–actuated formation of water–in–silicone oil DE as shown in Fig. 123.53. Two silicone oil droplets were first dispensed from the left reservoir through DEP by applying 330-V_{rms}, 100-Hz ac voltage on the lower array of electrodes. Then, two DI water droplets were dispensed from the right reservoir through EWOD actuation by application of 85-V_{rms}, 100-Hz ac voltage on the upper array of electrodes. With the same EWOD actuation voltages, the water droplets were then transported toward the oil droplets as shown in Figs. 123.53(c) and 123.53(d). After the water droplets touched the oil droplets, they were engulfed by the oil droplets to form DE droplets [see Fig. 123.53(e)]. Furthermore, the water droplets were able to pull the whole merged water-in-oil DE droplets by low-voltage EWOD transport [Fig. 123.53(f)].

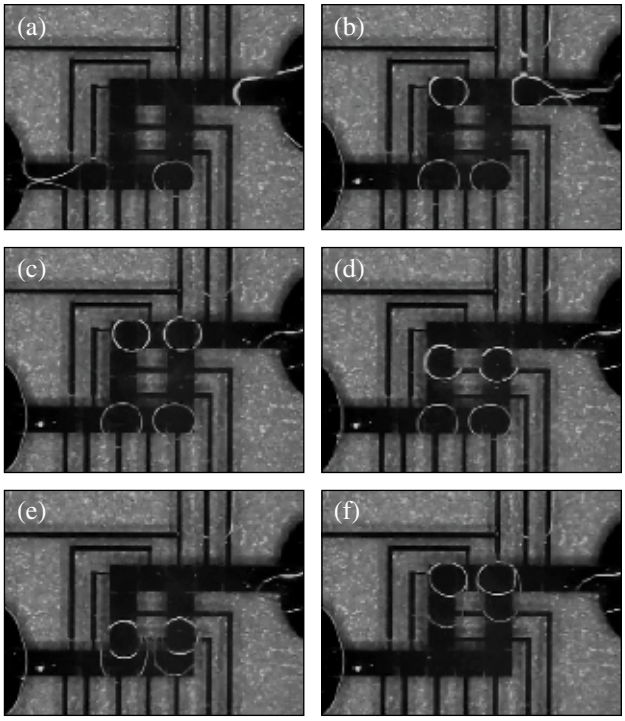

E18616JR

Figure 123.53
The formation of water-in-silicone oil DE droplets. (a) Two silicone oil droplets are dispensed through DEP actuation by applying 330-V_{rms}, 100-Hz ac voltage; (b) two DI water droplets are dispensed by EWOD actuation by applying 85-V_{rms}, 100-Hz ac voltage; [(c)–(e)] the water droplets are delivered and combined with oil droplets to form DE droplets; (f) the water droplets drag merged water-in-oil DE droplets by EWOD actuation.

3. Experiments for Oil-in-Water DE Formation.

We performed dispensing experiments with Silwet-treated water solutions of five wide ranging concentrations: 0.00625, 0.0125, 0.025, 0.0625, and 0.125 wt%. Only the 0.00625-wt% Silwet solution could be dispensed smoothly. All the others formed a remarkably persistent "tether" during the pinch-off process. As shown in Fig. 123.54(a), the thin liquid tether is formed between the reservoir and the droplet, preventing its separation. A full understanding of the tether formation is still lacking, but similar experiments in oil media show that surfactant-treated water can be successfully dispensed without tether formation.[10,11]

One way to break the tether is to use a second liquid finger to disturb it; this mechanism is shown in Fig. 123.54. The secondary liquid used was pure DI water. When the pure-water finger touches the tether, the Silwet solution in the contact area is diluted locally and the tether breaks because of the increased surface tension. The entire tether disintegrates into many satellite droplets because of hydrodynamic instability [see Fig. 123.54(d)].

This method does not work when the Silwet concentration exceeds 0.125 wt%, in which case the second water finger seems to mix with the tether instead of breaking it. Apparently the local dilution is not sufficient to increase the surface tension when the Silwet concentration is far above critical micelle concentration. Another problem with the tether formed during dispensing is that

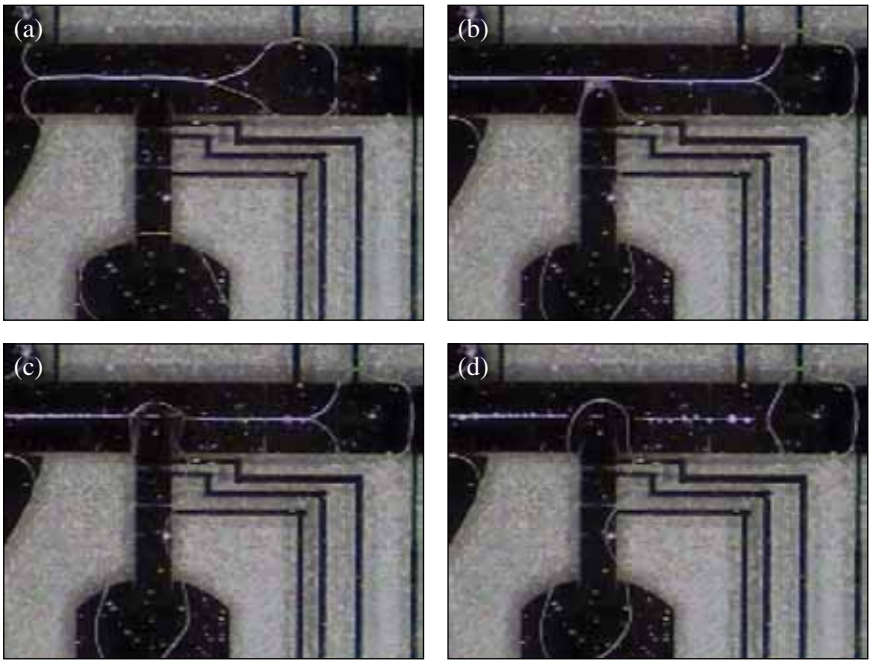

E18703JR

Figure 123.54
Breaking the tether with a second water liquid finger. (a) The second liquid (DI water) in a reservoir; (b) the second liquid finger approaches the "tether"; (c) the tether breaks inside the second liquid finger; (d) the entire tether disintegrates into many satellite droplets.

the electrode shape loses some of its influence in defining the pinch-off curvature, resulting in a poor volume reproducibility.

4. Other Possible Solutions to the Tether Problem

A second method to avoid the tether is by taking advantage of the pH effect on spreading of Silwet solutions. Radulovic[21] found that the wetting ability of Silwet solutions is drastically reduced with the addition of acetic acid, possibly because of the polarization of the trisiloxane head. We also found in experiments that the Silwet surfactant could be strongly affected by the addition of other acids (such as HCl) or bases (such as KOH), and the change in wetting ability by the pH effect is reversible by neutralization. In our work, we have demonstrated that the addition of acid to Silwet-treated water can prevent the tether formation. Then, the dispensed droplet is neutralized by mixing with another base droplet. In this way, the required low surface tension is recovered. The droplet now containing some salts can be used for oil-in-water DE's. The problem with this method is that the reversal process using a base solution takes a long time, typically more than an hour. This waiting time would be a major disadvantage for mass production of DE droplets. Also, evaporation of water during such a long period must be prevented.

A third approach would be to add the surfactant to the oil to avoid tether formation. We have found that Silwet has little influence on the wetting property of oils and Silwet-doped oil can be dispensed smoothly. When a pure water droplet and a Silwet-doped oil droplet are placed together, an oil-in-water DE droplet is formed because Silwet tends to stay in water phase. Unfortunately, the DE droplet formation takes some time because the Silwet diffuses gradually across the interface from the oil phase into the water phase. Using 0.125% (v/v) Silwet–added mineral oil and DI water droplets, the process takes several minutes. When a 0.5% (v/v) Silwet–modified mineral oil drop is used, the diffusion time is reduced to about 10 s.

Conclusion

In this article, we have demonstrated that aqueous and non-aqueous liquid droplets can be dispensed from reservoirs on a microfluidic chip and the dispensed droplets can then be combined to form oil-in-water-in-air (O/W/A) or water-in-oil-in-air (W/O/A) DE droplets. In the dispensing process, droplet volume reproducibility has been tested over a range of operational parameters, including applied voltage and the length of the cutting electrode. We find that drop volume variability is caused mainly by variability in the tail volume during pinch-off. When the length of the cutting electrode is increased, volume reproducibility is degraded because longer cutting electrodes reduce the influence of the electrode structure on the radius of curvature in the pinch-off region.

The Gibbs free energy change can be used to test the ability to form stable DE droplets. The result indicates that (1) water-in-oil DE droplets form through spontaneous emulsification and (2) oil-in-water DE droplets can also be formed by the addition of surfactant and the proper selection of oil. Experimental results show the formation of water-in-oil DE droplets. Using simultaneous DEP and EWOD actuation on a microfluidic chip, dielectric (oil) and conductive (water) droplets have been dispensed, and merged, and the transport of the merged water-in-oil DE droplet has been demonstrated.

The formation of water DE droplets treated with mineral oil–in–Silwet has been demonstrated. We find that a tether is formed during the dispensing of Silwet-treated water. Although the tether can be broken by the disturbance of a second liquid finger, it interferes with the dispensing operation and degrades dispensing reproducibility. Other methods to avoid the tether include taking advantage of the pH effect on Silwet solutions and adding the surfactant to the oil phase. Further effort to develop a more reliable formation method for oil-in-water DE is needed; for example, a surfactant more sensitive to pH might react more quickly so that its recovery of wetting ability (the contact angle reversal) would take much less time. Alternatively, low-surface-tension water could be dispensed in an oil medium without forming a tether. These schemes will be tested for oil-in-water DE formation.

ACKNOWLEDGMENT

This work was supported by the U.S. Department of Energy Office of Inertial Confinement Fusion under Cooperative Agreement No. DE-FC52-08NA28302, the University of Rochester, and the New York State Energy Research and Development Authority. The support of DOE does not constitute an endorsement by DOE of the views expressed in this article.

Appendix A: Requirements on DE Droplet Uniformity for Laser-Target Fabrication

The foam shell structure of a concentric laser target is shown in Fig. 123.55. V_1 and V_2 are the volumes of the inner oil phase and the outer water phase, respectively:

$$V_1 = \frac{4\pi}{3} R_1^3 \text{ and } V_1 + V_2 = \frac{4\pi}{3} R_2^3.$$

The shell thickness is $d = R_2 - R_1$; therefore, d can be written

$$d = \frac{\left(\frac{3}{\pi}\right)^{1/3} \cdot (V_1 + V_2)^{1/3}}{2^{2/3}} - \frac{\left(\frac{3}{\pi}\right)^{1/3} \cdot V_1^{1/3}}{2^{2/3}}. \quad \text{(A1)}$$

By taking partial derivatives of Eq. (A1), we obtain an expression for the uncertainty of d in terms of the uncertainties of V_1 and V_2

$$\Delta d = \left| \Delta V_1 \cdot \left[\frac{1}{6^{2/3}\pi^{1/3}(V_1+V_2)^{2/3}} - \frac{1}{6^{2/3}\pi^{1/3}V_1^{2/3}} \right] \right| + \left| \Delta V_2 \cdot \frac{1}{6^{2/3}\pi^{1/3}(V_1+V_2)^{2/3}} \right|. \quad \text{(A2)}$$

The specified dimensions of an inertial fusion energy (IFE) target are $2R_2 = 4 \pm 0.2$ mm, $d = 289 \pm 20$ μm. By substituting these values into Eq. (A2), we can determine wall-thickness variation ($\Delta d/d$) in terms of water and oil volume variations ($\Delta V/V$) (refer to Fig. 123.56). Different wall thickness variations ($\Delta d/d$) are represented by a set of straight lines in the $\left(\Delta V_1/V_1\right)$ versus $\left(\Delta V_2/V_2\right)$ chart. These lines have the same slope, and small ($\Delta d/d$) lines are closer to the original point. The shaded area indicates where the requirement on wall thickness variation is satisfied, i.e., $\Delta d/d < 20/289 = 6.92\%$. For example, if the oil volume variation $\left(\Delta V_1/V_1\right)$ is 5% and the water volume variation $\left(\Delta V_2/V_2\right)$ is 4%, the corresponding point indicated by a star in Fig. 123.56 is located within the shaded area, which means the wall thickness condition meets the requirement.

The red line in Fig. 123.56 represents where the changes of water- and oil-phase absolute volumes are the same, and the blue line represents where the relative volume variations of water and oil phases are the same. Under the condition of identical relative volume variations, $\left|\Delta V_1/V_1\right| = \left|\Delta V_2/V_2\right|$ must be smaller than 4.97% to meet the laser target requirement.

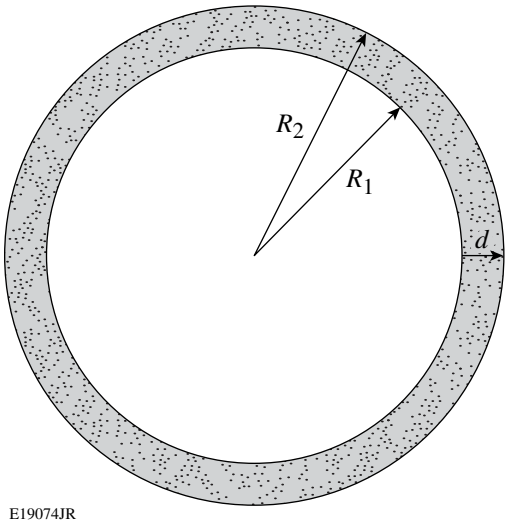

E19074JR

Figure 123.55
The foam shell structure of a concentric laser target.

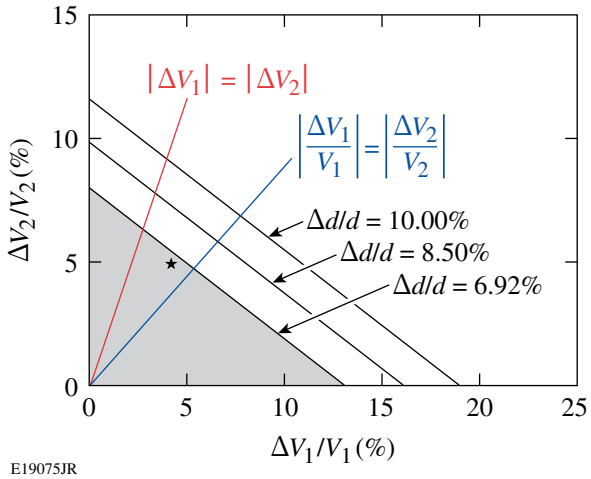

E19075JR

Figure 123.56
Sensitivity analysis of shell wall thickness for an IFE target.

REFERENCES

1. S. M. Lambert *et al.*, J. Appl. Polym. Sci. **65**, 2111 (1997).
2. R. Paguio *et al.*, in *Assembly at the Nanoscale—Toward Functional Nanostructured Materials*, edited by C. S. Ozkan *et al.*, Mat. Res. Soc. Symp. Proc. Vol. 901E (Materials Research Society, Warrendale, PA, 2006), Paper 0901-Ra05-23-Rb05-23.
3. N. Pannacci *et al.*, Phys. Rev. Lett. **101**, 164502 (2008).
4. A. S. Utada *et al.*, Science **308**, 537 (2005).
5. S. Okushima *et al.*, Langmuir **20**, 9905 (2004).
6. R. B. Fair, Microfluid Nanofluid **3**, 245 (2007).
7. T. B. Jones, Langmuir **18**, 4437 (2002).
8. M. G. Pollack, R. B. Fair, and A. D. Shenderov, Appl. Phys. Lett. **77**, 1725 (2000).
9. S. K. Cho, H. Moon, and C.-J. Kim, J. Microelectromech. Syst. **12**, 70 (2003).

10. H. Ren, R. B. Fair, and M. G. Pollack, Sens. Actuators B, Chem. **98**, 319 (2004).

11. J. Berthier *et al.*, Sens. Actuators A, Phys. **127**, 283 (2006).

12. R. B. Fair *et al.*, in IEEE International Electron Devices Meeting (IEDM 2003) (IEEE, New York, 2003), pp. 32.5.1–32.5.4.

13. T. B. Jones and M. Washizu, J. Electrostatics **37**, 121 (1996).

14. P. R. C. Gascoyne and J. V. Vykoukal, Proc. IEEE **92**, 22 (2004).

15. D. Chatterjee *et al.*, Lab Chip **6**, 199 (2006).

16. S.-K. Fan, T.-H. Hsieh, and D.-Y. Lin, Lab Chip **9**, 1236 (2009).

17. T. B. Jones, K.-L. Wang, and D.-J. Yao, Langmuir **20**, 2813 (2004).

18. K.-L. Wang and T. B. Jones, J. Micromech. Microeng. **14**, 761 (2004).

19. M. Bienia *et al.*, Physica A **339**, 72 (2004).

20. A. Staicu and F. Mugele, Phys. Rev. Lett. **97**, 167801 (2006).

21. J. Radulovic, K. Sefiane, and M. E. R. Shanahan, J. Colloid Interface Sci. **332**, 497 (2009).